Released 9/5/02 [illegible]

MEMORANDUM FOR: SAF/PAS
1690 Air Force Pentagon - 5D227
Washington DC 20330-1690

AUG 16 2002

FROM: Francis G. Hinnant, Col, USAF
Associate Director of Acquisition
NPOESS Integrated Program Office
8455 Colesville Rd, Suite 1450
Silver Spring, MD 20910

SUBJECT: Paper approval for: OMPS Total Column Algorithm Performance: Comparison to TOMS and to NPOESS Requirements

Enclosed are the required ten (10) copies of the subject papers. This paper will be released at the SPIE (International Society for Optical Engineering) International Asia-Pacific Environmental Remote Sensing Symposium to be held in Hangzhou, China on October 23 - 27, 2002. It was authored and will be presented by employees of Raytheon Information Technology and Scientific Services, Swissler InfoTech, Ball Aerospace & Technologies Corporation, and Science Systems and Applications, Inc.

The program office has reviewed the information in the attached papers and found it appropriate for public disclosure without change.

Point of contact on this matter is James W. Morris, NPOESS IPO/ADA at 301-427-2084 (Ext. 138).

Attachment: Presentation—10 copies

OMPS Total Column Algorithm Performance: Comparison to TOMS and to NPOESS Requirements

C.J. Seftor,*[1] J.C. Larsen[1], T.J. Swissler,[2] J.V. Rodriguez,[3] Q. Remund,[3]
G. Jaross,[4] C.G. Wellemeyer[4]
[1]Raytheon Information Technology and Scientific Services; [2]Swissler InfoTech;
[3]Ball Aerospace & Technologies Corp; [4]Science Systems and Applications, Inc.

ABSTRACT

One of the objectives of the National Polar-orbiting Operational Environmental Satellite System (NPOESS) program is to continue the long-term data set of total column ozone measurements from the Total Ozone Mapping Spectromenter (TOMS) systems while providing the increased accuracy and precision required by the NPOESS Integrated Program Office (IPO). In developing an Ozone Mapping and Profiler Suite (OMPS) sensor-algorithm system to meet the NPOESS requirements, we systematically analyzed the performance of the TOMS system and determined that it provided a strong starting point for the design of the OMPS system. In fact, our analysis showed that modern TOMS systems meet the NPOESS accuracy requirements for retrievals below 475 Dobson Units (DU). However, the NPOESS precision requirements are met only for retrievals below 225 DU. In order to meet the NPOESS accuracy and, particularly, precision requirements for all total column ozone amounts, we identified areas where improvements in the heritage design lead to the improved performance needed for the OMPS system. Simulations performed using the OMPS system design confirm that the algorithm enhancements, coupled with improvements contained in the OMPS sensor, provide performance that meets the NPOESS IPO requirements.

Keywords: NPOESS, OMPS, Ozone, Retrieval, Algorithm

1. INTRODUCTION

The over twenty-year (1978 – present) data set of measurements obtained by the various TOMS sensors (Nimbus-7, Meteor-3, ADEOS, and Earth Probe) forms the cornerstone of any satellite-based study of long-term ozone trends. Since the TOMS system onboard the Earth Probe satellite is the last of the series scheduled to fly, a new generation of total ozone mapping sensors is being developed to extend the long-term data set into the future. The Ozone Monitoring Instrument (OMI) is a sensor built by the Netherlands that is scheduled to be launched on NASA's EOS-Aura platform in 2004, while a series of OMPS sensors will be flown onboard the NPOESS platforms starting in 2008. These sensor-algorithm systems are designed to continue the measurement data set begun by Nimbus-7/TOMS, but with more stringent accuracy and requirements than any of the total column ozone retrieval systems currently in orbit. In particular, the OMPS system is required to meet an accuracy of 15 Dobson Units (DU), with a future objective of 5 DU, and a precision of 3 DU + 0.5% of total ozone amount, with a future objective of 1 DU.

In order to design a system to meet the NPOESS-OMPS requirements, we systematically reviewed the heritage TOMS sensor-algorithm system and developed error budgets for this system based on the NPOESS definitions of accuracy and precision. We then used our analysis to point to areas where enhancements in system design would lead to improvements that would bring the OMPS system to within the requirements required by the NPOESS program.

In this paper we first provide a brief review of the TOMS system and provide our error budget analysis for it. Next, we describe OMPS sensor and algorithm design enhancements that improve overall system performance and provide an OMPS error budget based on these enhancements. Finally, we provide results of simulations showing that the expected performance of the OMPS sensor-algorithm system meets, and often exceeds, the NPOESS requirements.

* seftor@hoss.stx.com; phone 1 301 794 5263; fax 1 301 794 3165; http://itss.raytheon.com; Raytheon ITSS, 4500 Forbes Blvd., Lanham, MD, 20706

2. THE TOMS SENSOR-ALGORITHM SYSTEM

2.1 TOMS sensor

The TOMS sensors use a single monochromator and scanning mirror to sample the backscattered solar ultraviolet radiation at six wavelengths. For Nimbus-7 and Meteor-3 TOMS, the six wavelengths selected for the sensor consisted of two strongly ozone absorbing (312 and 317 nm), one weakly ozone absorbing (331 nm), and three ozone non-absorbing (340, 360, and 380 nm). The six wavelengths selected for ADEOS and Earth Probe TOMS were changed to include three strongly ozone absorbing (308, 312, and 317 nm), two weakly absorbing (322 and 331 nm), and one ozone non-absorbing (360 nm).

Details on the TOMS sensors can be found in McPeters et al. [1996, 1998].

2.2 TOMS Version 7 algorithm

The TOMS Version 7 algorithm uses the ratio of measured radiance and solar flux, known as the normalized radiance (NR). The retrieval of ozone is based on a comparison between the measured NR's and NR's derived by radiative transfer calculations for different ozone amounts using the conditions of the measurement. The calculated NR's are based on a simplified Beer's law model of the atmosphere that includes Rayleigh scattering and ozone absorption:

$$I = Fe^{-s(\alpha\Omega+\beta p)} \quad ; \quad NR = \frac{I}{F} = e^{-s(\alpha\Omega+\beta p)} \tag{1}$$

where

I = Radiance
F = Solar Flux
Ω = Total column ozone amount
s = Path length = $\sec\theta_0 + \sec\theta$ (where θ_0 is the solar zenith angle and θ is the satellite zenith angle)
α = Ozone absorption coefficient
β = Rayleigh scattering coefficient
p = Pressure

The N value can then be defined as

$$N = -100\log_{10} NR = 100(s\beta p + s\alpha\Omega) = C_1\Omega + C_2 \tag{2}$$

Due to the above linearity, the comparison of measured to calculated values are done through interpolation using tables of N values. In practice, the algorithm compares the measured and calculated difference in N values for a pair of wavelengths, one strongly ozone absorbing and one weakly ozone absorbing. The use of such wavelength pairs greatly reduces wavelength-independent calibration effects.

Rather than deriving a total ozone value by interpolation of NR as a function of ozone, one can also reverse the process and use the tables to obtain the NR's that would be expected for a given column ozone and conditions of the measurement. The logarithm of the ratio of the measured NR to this calculated NR (or the difference between measured and calculated N values) is the residue.

The reflecting surface used to determine the calculated NR's is assumed to consist of two components, a surface component of lower reflectivity and a cloud component of higher reflectivity. By comparing the measured radiance at an ozone-insensitive wavelength with that calculated for cloud and for ground reflection alone, an effective cloud fraction can be determined and the contribution from each level can be derived:

$$f_{cld} = \frac{I_{meas} - I_{grd}}{I_{cld} - I_{grd}} \tag{3}$$

where

I_{meas} = the measured normalized radiance
I_{grd} = a normalized radiance calculated at the surface
I_{cld} = a normalized radiance calculated for a cloud

An initial ozone estimate is then derived using the effective cloud fraction and the difference between N values measured by the 317 and 331 nm wavelengths. This estimate is used to calculate residues for a second pair of wavelengths that are chosen to be those most sensitive to ozone at the optical path length, $s\Omega$, of the measurement. Table 1 shows the wavelength pairs used for the different TOMS systems.

Table 1: Wavelength pairs used in TOMS Version 7 algorithm

sΩ	**Nimbus-7 TOMS**	**Meteor-3 TOMS**	**ADEOS TOMS**	**Earth Probe TOMS**
$s\Omega \leq 1$	312 – 331	312 – 331	312 – 331	312 – 331
$1 < s\Omega \leq 3$	317 – 331	317 – 331	317 – 331	317 – 331
$s\Omega \geq 3$	331 – 340	331 – 340	322 – 331	322 - 332

In the absence of other geophysical phenomena or calibration errors, the residues should be zero. Consequently, non-zero values of the residues signify that either calibration errors or geophysical phenomena are not yet taken into account. The TOMS Version 7 algorithm corrects for such errors by assuming that the residue dependence is linear with wavelength, which adds a linear term to the Taylor series expansion about the initial ozone estimate:

$$N_m = N_0 + (\Omega - \Omega_0)\frac{dN}{d\Omega} + a + b\lambda \tag{4}$$

Since Equation 4 has three unknowns (a, b, and Ω), a wavelength triplet consisting of the chosen wavelength pair and the reflectivity wavelength is needed to solve for the final total column ozone amount, Ω.

3. TOMS ERROR BUDGET

3.1 TOMS accuracy

In determining an overall accuracy error budget corresponding to the original TOMS sensor-algorithm system on the Nimbus-7 satellite, the individual error sources were broken down into sensor and algorithm components. In order to obtain error estimates for each component we reviewed the latest published information concerning Nimbus-7/TOMS retrievals. We also performed simulations in support of OMPS development. Table 2 provides a list of each error component along with the references used to obtain the error estimate for that component.

3.2 TOMS precision

The overall precision error budget for the TOMS system was broken down in a similar fashion as the accuracy budget. Since the NPOESS definition of precision is based on a global ensemble of, we also needed to define such an ensemble. We based the ensemble on the following conditions:

1) Temperature variation is assumed to be the same for all ozone profiles;
2) Tropospheric aerosols are assumed to cover 10% of the Earth's surface (see Herman et al. [1997]);

Table 2: Sources of accuracy errors, references, and values corresponding to the Nimbus-7. For the first part of the table, the errors refer to the sensor, in the second the errors refer to the algorithm.

Source	Based on	Error	Ozone error
Sensor			
Wavelength independent albedo calibration	Wellemeyer et al. [1996]	2.0 %	0.3 %
Wavelength dependent albedo calibration	Jaross et al. [1998]	0.7 %	4.9 DU
Long-term wavelength independent albedo calibration	Wellemeyer et al. [1996]	0.7 %	0.7 DU
Long-term wavelength dependent albedo calibration	Wellemeyer et al. [1996]	0.7 %	0.10 %
Linearity	Analysis of TOMS data (see OMPS ATBD)	0.2 %	1.4 DU
Wavelength calibration accuracy	Wellemeyer et al. [1996]	0.07 nm	3.50 %
On-orbit wavelength shift sensitivity	Simulations with TOMS wavelength triplets	0.002 nm	0.10 %
Polarization sensitivity	Jaross et al. [1995]	4.0 %	0.10 %
Stray light (out-of-field)	Analysis of TOMS data (see OMPS ATBD)	0.1%	0.01 %
Stray light (out-of-band)	N7/TOMS sensor requirement	0.5 %	3.0 DU
Algorithm			
Rayleigh scattering coefficient	Fleig et al. [1990]	0.3 %	0.30 %
Ozone absorption coefficients	Qu et al. [2000]	1.0 %	1.00 %
Aerosol correction	Torres et al. [1999]	-	0.80 %
Ring effect correction	Joiner et al. [1995]	-	0.20 %
Cloud top pressure	Wellemeyer et al. [2000]	100 mbar	1.52 %
Pressure table interpolation	Simulations using TOMS tables	-	1.25 %
Ozone profile shape	Wellemeyer et al. [1997]	-	1.00 %
Temperature	McPeters et al. [1996]	-	1.00 %
Multiple scattering	Klenk et al. [1982]	-	0.20 %

3) SNR and profile shape are based on the distribution of solar zenith angles for an orbit with a 09:30 local equator crossing time; this time was chosen to represent the worst case scenario for an NPOESS orbit
4) Ozone amounts are based on a distribution determined from the 14.5 year Nimbus-7/TOMS data set and shown in Figure 1a; and
5) Cloud top pressure and tropospheric pressure are based on a cloud fraction distribution determined from the Nimbus-7 TOMS data set and shown in Figure 1b.

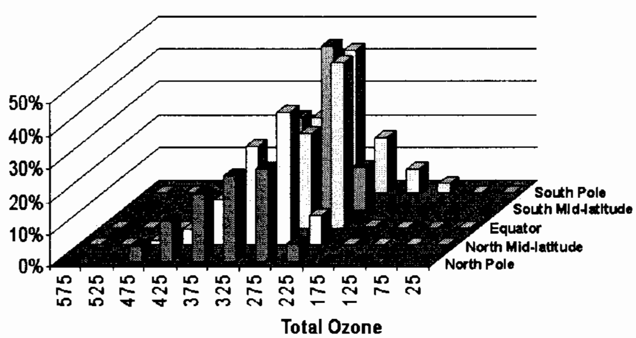

Figure 1a: The global distribution of total column ozone amount from the 14.5 year Nimbus-7 TOMS data set.

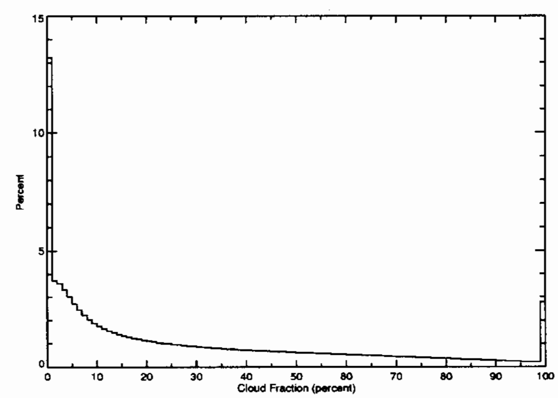

Figure 1b: The global distribution of cloud fraction from one year (1979) of Nimbus-7 TOMS data. Different years show similar distributions.

The terms, error estimates for each term, and the references used to obtain the error estimate for that component are presented in Table 3.

Table 3: Sources of precision errors, references, and values corresponding to the Nimbus-7 TOMS system

Source	Based On	Error for different SZA regions		
		< 60°	60-70°	> 70°
Radiance SNR	McPeters et al [1996]	0.3%	0.3%	0.3%
Solar calibration	Jaross et al. [1998]	0.2%	0.25%	0.33%
Temperature dependence	McPeters et al [1996] / simulations for OMPS	1.0%	1.0%	1.0%
Cloud top pressure	Wellemeyer et al. [1997] / simulations for OMPS	1.5%	1.5%	1.5%
Ozone profile shape	Wellemeyer et al. [1997]	0.1%	0.1%	1.0%
Aerosol correction	Torres et al. [1999]	0.5%	0.5%	0.5%
Tropospheric ozone	TOMS User's Guide [1998] / simulations for OMPS	1.5%	1.5%	1.5%

A plot of the accuracy error budget values as a function of ozone amount is shown in Figure 2a. The algorithm errors are plotted separately from the total Nimbus-7 system errors. Also plotted is the total error budget for a more recent TOMS system being flown on the Earth Probe satellite. Since the algorithm and sensor are the same for both instruments, the large difference in total error between the two systems reflects differences in calibration. In particular, the pre-launch wavelength calibration of Earth Probe TOMS was much more accurate (with an uncertainty of 0.01 nm instead of 0.07 nm), which leads to the major portion of the difference between the two systems. Figure 2a shows that, for current TOMS systems like the one being flown on Earth Probe, the accuracy performance is within NPOESS requirements below 475 DU which, as shown in Figure 1a, constitute most of the measurements within the atmosphere. This analysis shows that current TOMS sensor-algorithm systems serve as a good basis for the development of OMPS.

In Figure 2b we show the results of combining our precision error estimates in Table 3 with the definitions of the global ensemble of measurements to obtain the total precision performance of the Nimbus-7/TOMS system. A similar analysis for Earth Probe TOMS indicated that the improved sensor performance of current TOMS systems (including improved SNR) results in only small improvements in the total precision estimate.

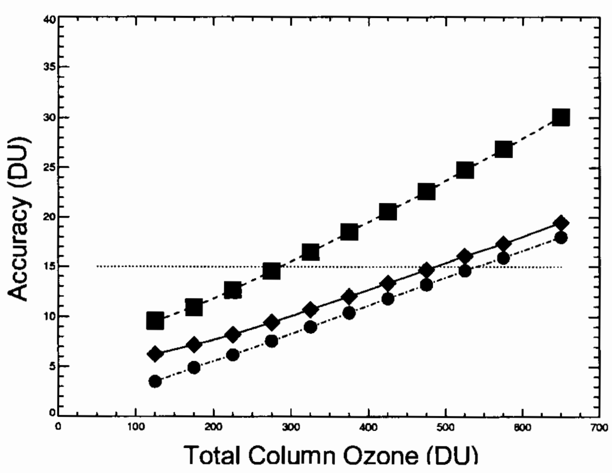

Figure 2a: Accuracy error analysis for the TOMS sensor-algorithm system. The dashed line is the Version 7 algorithm, the chain-dashed line is the total Nimbus-7 system, and the solid line is the total Earth Probe system. The dotted line represents the NPOESS original threshold requirements

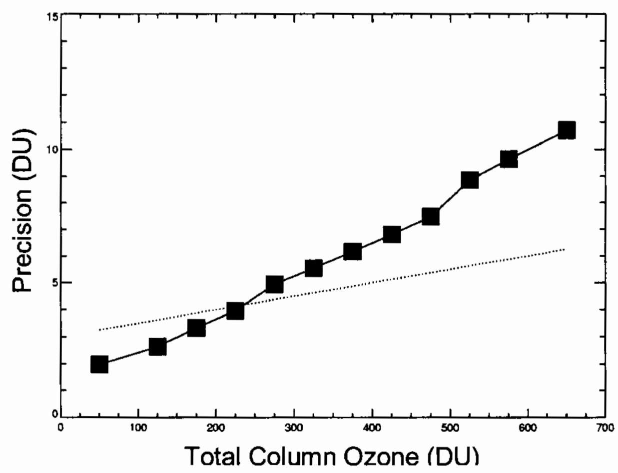

Figure 2b: Precision error analysis for the TOMS system. The dotted line represents the NPOESS original threshold requirements.

4. OMPS ENHANCEMENTS RELATED TO ACCURACY

4.1 Hyperspectral sensor

A comparison of the TOMS algorithm error curve with the EP total error curve in Figure 2a indicates that improvements in the sensor directly lead to only small improvements in accuracy performance. Indirectly, however, sensor design improvements do allow for major improvements in algorithm design and in calibration, leading to larger improvements in accuracy performance.

For example, the hyperspectral design of the OMPS sensor means that the algorithm can select wavelengths to minimize the effects of temperature, Raman scattering, and O_2-O_2 absorption. Furthermore, the use of multiple triplets in a single retrieval decreases the algorithm's sensitivity to wavelength shift errors.

4.2 Use of external data

External information on ozone profile from the OMPS limb sensor and temperature profile data from the NPOESS-CrIS system are used to correct for the errors in climatological profile shape introduced by using climatological ozone and temperature profiles in the lookup tables. The corrections are made by incorporating the information in a Taylor series expansion about the Version 7 ozone estimate, Ω_0:

$$N = N_0 + (\Omega - \Omega_0)\frac{dN}{d\Omega} + \sum_{lyr}(x - x_0)_{lyr}\frac{dN}{dx_{lyr}} + \sum_{lyr}(t - t_0)_{lyr}\frac{dN}{dt_{lyr}} \tag{5}$$

where

x_0 = Layer ozone amount from OMPS
t_0 = Layer temperature amount from CrIS
x = Standard layer ozone used in OMPS N value table
t = Standard layer temperature amounts used OMPS N value table

4.3 Improved pressure table interpolation

The addition of higher pressure node points in the N value table prevents extrapolation off the end of the table that results in ozone errors as large as 3% over mid-latitude high clouds (such as those found in thunderstorms) and as large as 1% for low-latitude high clouds. A switch from linear to polynomial interpolation further reduces the error to 0.2% for all pressure levels.

Table 4 provides the resulting error budget for the OMPS sensor with these improvements in place, while a plot of the root-sum-squared error as a function of total ozone amount is shown in Figure 3a. The OMPS accuracy performance meets the NPOESS threshold requirements.

5. OMPS ENHANCEMENTS RELATED TO PRECISION

5.1 Tropospheric ozone correction

The results shown in Table 3 indicate that, along with cloud top pressure, errors due to the uncertainty in tropospheric ozone amount have the largest effect on the precision estimate. The use of the ozone profile from the OMPS limb retrieval sensor-algorithm system allows us to incorporate an improved tropospheric residual technique (see Fishman et al. [1996]) into the algorithm to determine a better estimate of the tropospheric ozone amount.

Table 4: Sources of accuracy errors, and values corresponding to the OMPS sensor-algorithm system

Source	Error	Ozone error
Sensor		
Wavelength independent albedo calibration	2.0 %	0.28 %
Wavelength dependent albedo calibration	0.5 %	0.02 %
Long-term wavelength independent albedo calibration	0.15 %	3.5 DU
Long-term wavelength dependent albedo calibration	0.25 %	1.75 DU
Linearity	0.5 %	3.5 DU
Wavelength calibration accuracy	0.015 nm	0.36 %
On-orbit wavelength shift sensitivity	0.01 nm	0.24 %
Polarization sensitivity	5.0 %	0.1 %
Stray light (out-of-field)	1.0 %	0.14 %
Stray light (out-of-band)	1.0 %	0.46 %
Algorithm		
Rayleigh scattering coefficient	0.1 %	0.1 %
Ozone absorption coefficients	1.0 %	1.0 %
Aerosol correction	-	0.8 %
Ring effect correction	-	0.2 %
Cloud top pressure	30 mbar	0.76 %
Pressure table interpolation	0.2 %	0.3 %
Ozone profile shape	-	0.5 %
Temperature	1 K	0.5 DU
Multiple scattering	-	0.2 %

The tropospheric residual, X_{res}, is defined as the difference between total column ozone amount estimated by the total column system and stratospheric ozone amount determined by summing up the OMPS limb-retrieved profile down to the tropopause,

$$X_{res} = \Omega - \sum_{strat} x_{limb} \tag{6}$$

where $\sum_{strat} x_{limb}$ is the sum of the limb ozone profile down to the tropopause. We call the difference between X_{res} and the amount of tropospheric ozone in the standard profile chosen by the table look up, and that corresponds to Ω, the tropospheric excess, X^0_{trop}.

If the nadir-mapping sensor were 100% efficient in measuring ozone in the troposphere, the tropospheric excess would be an accurate measure of the difference between the actual amount of tropospheric ozone and X^0_{trop}, and the tropospheric residual would be an accurate measure of the tropospheric ozone amount. Also, although the total ozone retrieval would be based on the wrong profile shape, the retrieved total ozone amount would still be correct.

Since the sensor is not 100% efficient in measuring tropospheric ozone, however, the tropospheric excess is not equal to the difference between actual and standard tropospheric ozone amounts. As a result, the tropospheric residual is not equal to the tropospheric ozone amount, and the retrieved total column ozone amount is incorrect. If we correct the tropospheric residual using an estimate of the measurement efficiency, ξ_{trop}, we then determine the correct difference between the actual amount of tropospheric ozone and the amount in the chosen standard profile:

$$Corrected\ tropospheric\ excess = \frac{X_{res} - X^0_{trop}}{\xi_{trop}} \tag{7}$$

We then write:

$$X_{trop} = \frac{X_{res} - X^0_{trop}}{\xi_{trop}} + X^0_{trop} \tag{8}$$

where X_{trop} is the actual amount of tropospheric ozone. We estimate the tropospheric efficiency as:

$$\xi_{trop} = \frac{\sum\limits_{trop} \xi_{layer}(x_{climatology} - x_{standard})}{\sum\limits_{trop}(x_{climatology} - x_{standard})} \tag{9}$$

where ξ_{layer} represents the measurement efficiencies in each atmospheric layer in the troposphere, $x_{standard}$ is the amount of ozone in a given tropospheric layer in the standard profile, and $x_{climatology}$ is the amount contained in a climatological database. One should note that the efficiency estimate is weighted by the vertical distribution in ozone differences between the climatology and the standard profiles and not on the total tropospheric ozone difference between the two.

The database consists of monthly tropospheric ozone amounts on a 1-degree longitude by 1-degree latitude grid. The initial contents have been generated using ozone profile information obtained using the UK Universities Global Atmosphere Modeling Program (UGAMP) ozone climatology (Li et al., 1995). This 4-dimensional (latitude, longitude, altitude, time) climatology was developed using ozone profile information from balloonsonde measurements and satellite measurements from SBUV, SBUV/2, MLS, and SAGE II. Total ozone information was obtained from TOMS instruments. Once the OMPS system is in orbit, the database will be updated as the nadir-mapping sensor determines more accurate tropospheric ozone values.

5.2 Use of external data from co-located sensors

Table 3 also indicates that errors in cloud top pressure result in precision errors for the TOMS sensors that are as large as those due to incorrect tropospheric ozone. As in the case of accuracy, the OMPS algorithm will use co-located cloud to pressure information from the NPOESS Visible Infrared Imager Radiometer Suite (VIIRS) system. As a result, cloud pressure uncertainty will be reduced from 100 mbar to 50 mbar. Beside cloud pressure, the use of other co-located data from other NPOESS sensors will reduce the uncertainty resulting from the use of climatologies in the TOMS system:

1) Use of the co-located ozone profile from the limb retrieval system will reduce the uncertainty from 1.0% to 0.5%
2) Use of temperature information from the NPOESS-CrIS system will reduce the uncertainty from 1% to less than 0.3% in most cases.

5.3 Use of multiple triplet retrievals

To reduce the effects of sensor noise, the total algorithm retrieval process is performed for each sensor measurement using 12 different sets of triplets. The cloud fraction is determined using 4 different ozone-insensitive wavelengths (364, 367, 372, and 377 nm). Then, each of these reflectivity wavelengths is matched to 3 different pairs of wavelengths that form the wavelength triplets used to determine ozone. Similar to the 3 wavelength triplets used for the TOMS systems, the choice of triplets depends on their ability to accurately measure ozone for the viewing conditions of the measurement or, in other words, their ozone sensitivity.

From Beer's Law we know that, for a given wavelength, λ:

$$I_\lambda = F_\lambda e^{-s(\alpha\Omega+\beta p)} \quad ; \quad NR_\lambda = \left(\frac{I}{F}\right)_\lambda = e^{-s(\alpha\Omega+\beta p)} \quad ; \quad \Delta NR_\lambda = -\alpha s e^{-s\alpha_\lambda \Omega}\Delta\Omega \quad ; \quad \frac{\Delta NR_\lambda}{NR} = -\alpha s \Delta\Omega \tag{10}$$

The wavelength sensitivity (percent change in albedo per percent change in ozone) is therefore

$$\frac{\Delta NR_\lambda / NR_\lambda}{\Delta\Omega / \Omega} = -\alpha s \Omega, \text{ or } \frac{\Delta NR_p / NR_p}{\Delta\Omega / \Omega} = -\Delta\alpha s\Omega \tag{11}$$

where p represents the wavelength pair. The quantity $\Delta\alpha s\Omega$ can therefore be used to assess the sensitivity of each ozone triplet.

Table 5 shows $\Delta\alpha s\Omega$ as a function of the path length $s\Omega$ for each of the wavelength pairs that are matched to the 4 reflectivity channels (the differential sensitivity is presented since the algorithm uses a pair of wavelengths matched to the reflectivity wavelengths).

Table 5: Selection of the Multiple Triplets for OMPS is based on $\Delta\alpha s\Omega$.

$s\Omega$ / λ Pairs	0.75	1.00	1.25	1.50	1.75	2.00	2.50	3.00	3.50	4.00	5.00	6.00
308.5 – 321.0	1.96	2.61	3.26	3.92	4.57	5.22	6.53	7.83	9.14	10.44	13.05	15.66
310.5 – 321.0	1.39	1.85	2.32	2.78	3.24	3.71	4.63	5.56	6.48	7.41	9.26	11.12
312.0 – 321.0	1.06	1.41	1.77	2.12	2.48	2.83	3.54	4.24	4.95	5.66	7.07	8.49
312.5 – 321.0	0.92	1.23	1.54	1.85	2.16	2.46	3.08	3.70	4.31	4.93	6.16	7.39
314.0 – 321.0	0.79	1.05	1.31	1.57	1.83	2.09	2.62	3.14	3.66	4.19	5.23	6.28
318.0 – 336.0	0.62	0.83	1.04	1.24	1.45	1.66	2.07	2.49	2.90	3.32	4.15	4.97
315.0 – 321.0	0.54	0.72	0.90	1.09	1.27	1.45	1.81	2.17	2.53	2.90	3.62	4.34
320.0 – 329.0	0.44	0.59	0.73	0.88	1.03	1.17	1.47	1.76	2.05	2.35	2.93	3.52
322.5 – 332.0	0.33	0.43	0.54	0.65	0.76	0.87	1.09	1.30	1.52	1.74	2.17	2.61
325.0 – 336.0	0.27	0.36	0.45	0.54	0.63	0.72	0.90	1.08	1.25	1.43	1.79	2.15
328.0 – 336.0	0.19	0.25	0.32	0.38	0.45	0.51	0.64	0.76	0.89	1.02	1.27	1.53
331.0 – 336.0	0.11	0.14	0.18	0.21	0.25	0.28	0.35	0.42	0.49	0.56	0.70	0.84
316.0 – 329.0	0.73	0.98	1.22	1.47	1.71	1.96	2.45	2.94	3.43	3.92	4.90	5.88
317.0 – 321.0	0.35	0.47	0.59	0.71	0.82	0.94	1.18	1.41	1.64	1.88	2.35	2.82

The clear area in the table indicates which wavelength pairs have ozone sensitivity needed to accurately determine ozone for each atmospheric condition. The path lengths across the top are the maxima for the corresponding bins. The use of multiple triplets reduces the SNR-related error to less than 0.2%. As mentioned earlier, the use of multiple triplets also reduces the effects of wavelength shifts.

A table of the resulting error budget with these improvements included for both the sensor and algorithm is shown in Table 6, with a corresponding plot of the total precision error as a function of total column ozone shown Figure 3b. As in the case of accuracy, the OMPS enhancements bring the precision performance to within the NPOESS requirements everywhere.

Table 6: Sources of precision errors and values corresponding to OMPS sensor-algorithm system.

Source	Total Column Ozone Amount (DU)											
	50	125	175	225	275	325	375	425	475	525	575	625
Radiance SNR	0.15	0.25	0.35	0.45	0.55	0.65	0.75	0.85	0.95	1.05	1.15	1.25
Solar calibration	0.15	0.25	0.35	0.45	0.55	0.65	0.75	0.85	0.95	1.05	1.15	1.25
Temp dependence	0.50	0.50	0.50	0.50	0.50	0.50	0.50	0.50	0.50	0.50	0.50	0.50
Cloud top pressure	0.28	0.47	0.66	0.78	0.96	1.13	1.31	1.48	1.66	1.99	2.18	2.37
Cloud fraction	0.23	0.38	0.53	0.68	0.83	0.98	1.13	1.28	1.43	1.58	1.73	1.88
Ozone profile shape	0.27	0.45	0.63	0.56	0.69	0.81	0.94	1.06	1.19	1.89	2.07	2.25
Aerosol correction	0.12	0.20	0.28	0.36	0.43	0.51	0.59	0.67	0.75	0.83	0.91	0.99
Tropospheric ozone	1.23	1.23	1.23	0.98	2.89	2.71	1.78	1.61	1.43	1.52	1.52	1.52

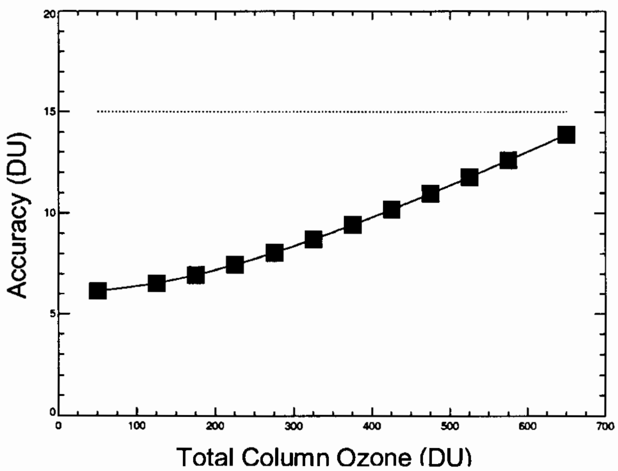

Figure 3a: Accuracy error budget for the OMPS sensor-algorithm system. Solid line is OMPS predicted performance and dashed line is NPOESS original threshold requirement.

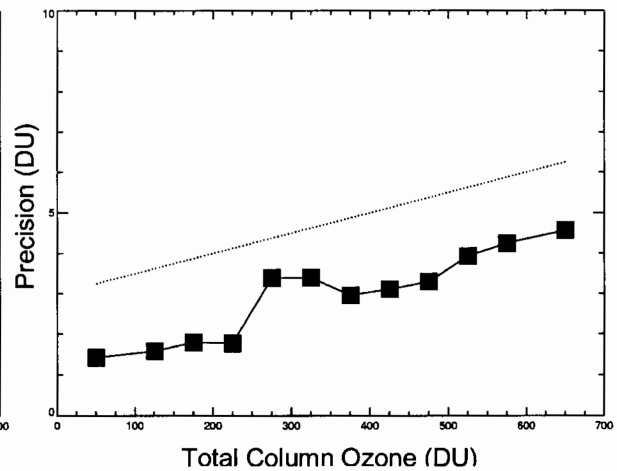

Figure 3b: Precision error budget for the OMPS sensor-algorithm system. Solid line is OMPS predicted performance and dashed line is NPOESS original threshold requirement.

6. VALIDATION

In order to validate our results, we performed two sets of simulations. In the first set, we compared the performance of the TOMS Version 7 algorithm to the performance of the OMPS algorithm. In the second, we performed a set of Monte Carlo simulations.

6.1 Comparison of TOMS and OMPS algorithms

To directly compare the performance of the TOMS and OMPS algorithms, we performed simulations using a set of ozone and temperature profiles provided by Larry Flynn of the NPOESS Ozone Operational Algorithm Team. We calculated normalized radiances for each of these of ozone and temperature profiles using our forward model radiative transfer code and assuming:

1) A solar zenith angle corresponding to a 13:30 local equator crossing time and time of year defined for each profile;
2) Six different satellite zenith angles for each of the profiles;

3) Four different relative azimuth angles for each pair of profiles; and
4) A perfect sensor.

Figure 4a shows the result for these 2184 pairs of retrievals using both the TOMS and OMPS algorithms. These results clearly indicate that the OMPS algorithm outperforms the heritage TOMS algorithm.

6.2 Monte Carlo simulations

To validate that the performance of the OMPS algorithm meets the NPOESS requirements, we performed a set of Monte Carlo simulations. In one example, we added 10 DU in the troposphere to the 325 DU standard ozone and temperature profile used to calculate N values in the OMPS table. We then ran a series of retrieval simulations using a solar zenith angle of 40°, a satellite zenith angle of 50°, a relative azimuth angle of 90°, and for 4 different reflectivities (0%, 20%, 50%, and 100%). For this series of simulations a set of 2000 normalized radiances were calculated for each reflectivity using our forward model radiative transfer code by randomly varying the following components of the retrieval error by their 1-sigma values as shown in Table 7. The 1-sigma values correspond to the values given for the OMPS and other NPOESS systems.

Table 7: 1-sigma values of error components

Error source	1-sigma value	Origin of 1-sigma value
SNR	1000	OMPS sensor requirement
Cloud pressure	30 mbar	VIIRS EDR uncertainty, h>7 km
Ozone profile	3 % of layer value	OMPS profile requirement, 15-50 km
Temperature profile	1 K of layer value	CrIS EDR requirement for p > 30mb

The results for the 0% reflectivity retrievals, shown in Figure 4b, clearly indicate that the 1-sigma value is well within the NPOESS precision requirement for this total ozone amount.

The 1-sigma values for all four reflectivities are shown in Table 8. Although the 1-sigma values are above the NPOESS requirement for reflectivities above 50%, analysis using the Nimbus-7/TOMS data set indicate that such conditions only occur 24% of the time. Furthermore, when the above 1-sigma values are applied to a global ensemble of measurements, the overall OMPS algorithm performance falls well within the NPOESS requirements.

Table 8: 1-sigma values of error components. Precision requirement for 325 DU is 4.4 DU. With reflectivity weighted according to a global ensemble basis, the predicted error is 3.2 DU.

Reflectivity	1-sigma value
0 %	2.6 DU
20 %	3.4 DU
50 %	4.7 DU
100 %	5.3 DU

6. CONCLUSIONS

Our analysis of the TOMS total column sensor-algorithm system showed that its performance already provided a strong baseline for the development of the OMPS total column system. By basing our design of the OMPS system in part on the TOMS V7 algorithm, we were able to combine the best attributes of this heritage system with enhancements that bring the performance of the next generation of total column systems within the stringent requirements required by the NPOESS program.

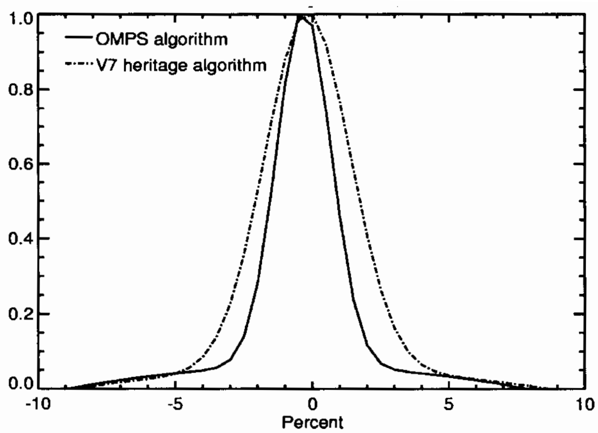

Figure 4a: Comparison of error distributions for retrievals using WPTB profiles with TOMS (dashed line) and OMPS (solid line) algorithms.

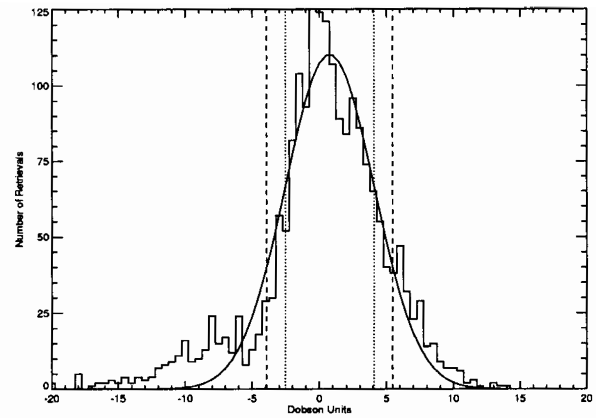

Figure 4b: Resulting errors from simulated retrievals using the OMPS algorithm. The dotted Lines represent 1-sigma performance, while the dashed lines represent the NPOESS requirements.

7. REFERENCES

1. Fishman, J., V.G. Brackett, E.V. Browell, W.B. Grant, "Tropospheric ozone derived from TOMS/SBUV measurements during TRACE A," *J. Geophys. Res., 101*, 24069-24082, 1996.
2. Fleig, A.J., et al., Nimbus 7 Solar Backscatter Ultraviolet (SBUV) Ozone Products User's Guide, *NASA Reference Publication 1234*, 1990.
3. Herman, J.R., P.K. Bhartia, O. Torres, N.C. Hsu, C.J. Seftor, and E. Celarier, Global distribution of absorbing aerosols from Nimbus-7/TOMS data, *J. Geophys. Res., 102*, 16911, 1997.
4. Jaross, G., et al., Calibration and postlaunch performance of the Meteor 3/TOMS instrument, *J. Geophys. Res., 100,* 2985—2995, 1995.
5. Jaross, G., A. J. Krueger, and C. G. Wellemeyer, Sensitivity of Total Ozone Mapping Spectrometer products to diffuse reflectance measurements, *Metrologia, 35,* 663-668, 1998.
6. Joiner, J., P. K. Bhartia, R. P. Cebula, E. Hilsenrath, and R. D. McPeters, Rotational-Raman Scattering (Ring Effect) in Satellite Backscatter Ultraviolet Measurements, *Appl. Opt., 34*, 4513-4525, 1995.
7. Klenk, K.F., P.K. Bhartia, A.J.Fleig, V.G. Kaveeshwar, R.D. McPeters, and P.M.Smith, "Total Ozone Determination from the Backscattered Ultraviolet (BUV) Experiment," *J. Appl. Meteor.*, 21, 1672-1684, 1982.
8. Li, D. and K. P. Shine, "A 4-Dimensional Ozone Climatology for UGAMP Models," UGAMP Internal Report No. 35, April, 1995.
9. McPeters, R.D., et al., "Nimbus-7 Total Column Ozone Mapping Spectrometer (TOMS) Data Product User's Guide," *NASA Reference Publication* 1384, National Aeronautics and Space Administration, 1996.
10. McPeters, R.D., et al., "Earth Probe Total Column Ozone Mapping Spectrometer (TOMS) Data Product User's Guide," *NASA Reference Publication* 1998-206895, National Aeronautics and Space Administration, 1998.
11. Seftor, C.J., et al., "Nadir Total Column Ozone Algorithm Theoretical Basis Document (ATBD) for the Ozone Mapping and Profiler Suite (OMPS) of the National Polar-Orbiting Operational Environmental Satellite System (NPOESS) Program, http://npoesslib.ipo.noaa.gov/atbd_omps.htm, 2002.
12. Torres, O. and P.K. Bhartia, "Impact of Tropospheric Aerosol Absorption on Ozone Retrieval from Backscattered Ultraviolet Measurements," *J. Geophys. Res.*, 104 D17, 21569-21577, 1999.
13. Wellemeyer, C.G., S.L. Taylor, G. Jaross, M.T. Deland, C.J. Seftor, G. Labow, T.J. Swissler, and R.P. Cebula, Final report on Nimbus-7 TOMS Version 7 calibration, *NASA Contractor Report 4717*, 1996.
14. Wellemeyer, C.G., S.L. Taylor, C.J. Seftor, R.D. McPeters, P.K. Bhartia, "A Correction for TOMS Profile Shape Errors at high latitudes," *J. Geophys. Res.*, 102, 9020, 1997.

15. Wellemeyer, C.G., C.J. Seftor, G. Jaross, P.K. Bhartia, "Evaluation of Errors in the Version 7 TOMS Algorithm," *Proceedings of the Quadrennial Ozone Symposium, Sapporo,*719-720, 2000.